ACADEMIA ROMÂNĂ
Revue Roumaine de Chimie
http://web.icf.ro/rrch/

Rev. Roum. Chim.,
2016, *61*(8-9), 657-663

Dedicated to Professor Claude Nicolau on the occasion of his 80th anniversary

EFFECTS OF PHOS-*b*-PMAA ADDITIVE AND pH ON THE FORMATION OF CALCIUM CARBONATE COMPOSITE MICROPARTICLES

Marcela MIHAI,[a] Grigoris MOUNTRICHAS,[b] Stergios PISPAS[b] and Bogdan C. SIMIONESCU[a,c,*]

[a] "Petru Poni" Institute of Macromolecular Chemistry of Romanian Academy, 41 A Grigore Ghica Voda Alley, 700487 Iaşi, Roumania
[b] Theoretical and Physical Chemistry Institute, National Hellenic Research Foundation, 48 Vassileos Constantinou Ave., 11635 Athens, Greece
[c] "Gh. Asachi" Technical University, Department of Natural and Synthetic Polymers, 73 Prof. Dimitrie Mangeron Street, 700050 Iaşi, Roumania

Received November 12, 2015

The influence of environmental pH on the crystallization of calcium carbonate microparticles from supersaturated aqueous solutions in the presence of poly(p-hydroxystyrene–*b*–methacrylic acid) PHOS-*b*-PMAA, was investigated. The formation of $CaCO_3$/PHOS-*b*-PMAA microparticles under different polymer concentrations at pH = 12, when both copolymer blocks are ionized, was compared to microparticles preparation at pH = 9.5, when only the PMAA block is ionized. The morphology of the composites was investigated by scanning electron microscopy and atomic force microscopy, and the polymorphs characteristics by X-ray diffraction and Raman spectroscopy. The particles mean size and circularity was followed by flow particle image analysis and the polymer presence into the composite particles was evidenced by thermogravimetric analysis, particles charge density and zeta potential.

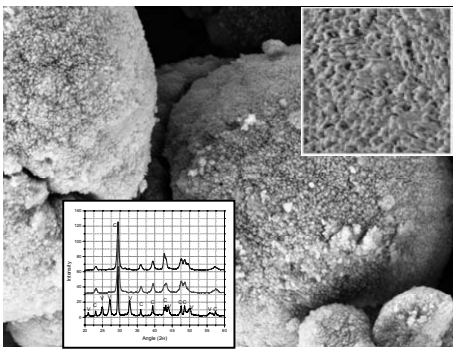

INTRODUCTION

Calcium carbonate is a common biomineral. As a result of its wide applications in different industries,[1,2] an extensive attention has been paid in the last decades to its mineralization mechanism and biomimetic synthesis. The $CaCO_3$ crystal growth and morphology depends on a number of parameters including pH, temperature, reaction time, stoichiometry of the reactants, concentration of additives and, for polymeric additives, the type of functional groups.[3-9]

Self-assembly is a powerful tool in forming complex structures of micro and nanoscale dimensions. Depending on the obtained morphologies (size, shape, periodicity, etc.) the self-assembled systems can be applied, or be of interest, for a number of applications in biomineralization, nanotechnology, drug delivery and gene therapy.[10-14] In this respect, amphiphilic block copolymers that self-organize in solution have been found to be very versatile.[11,12,15] Double-hydrophilic block copolymers (DHBC) can be also used as templates for the effective control of the

* Corresponding author: bcsimion@icmpp.ro

morphology of inorganic crystals.[12,16] In a previous study, the crystallization of $CaCO_3$ as composite microparticles in the presence of poly(p-hydroxystyrene–*b*–methacrylic acid), PHOS-*b*-PMAA, was described.[17] The study highlighted both the possibilities and the limitations of $CaCO_3$/PHOS-*b*-PMAA microparticles formation under different inorganic/polymer relative ratios, controlled by initial solution supersaturation and polymer concentration. However, at the tested pH (~9.5) only the PMAA bocks are ionized and actively participate to crystal nucleation and growth. Therefore, the aim of this study is to follow $CaCO_3$/PHOS-*b*-PMAA microparticles formation under different polymer concentrations, at pH = 12 where both copolymer blocks are ionized. The morphology of the new composites was investigated by scanning electron microscopy (SEM) and atomic force microscopy (AFM). The polymorphs characteristics were determined by X-ray diffraction and Raman spectroscopy. Particles mean size and circularity was followed by flow particle image analysis (FPIA), whereas the polymer presence into the composite particles was evidenced by thermogravimetric analysis (TGA), particles charge density and zeta potential measurements.

RESULTS AND DISCUSSION

Previous results[17] showed that using 0.2 M calcium and carbonate ions concentration in the starting solutions ensures the best conditions to prepare composite particles by using PHOS-*b*-PMAA, taking into account the particles organic/inorganic distribution, and surface charge density. The polymer additive used in this study is pH sensitive, both blocks having different functional groups, with different pK_as. As previously shown,[15] the PMAA and PHOS blocks present two equivalent points, ascribed to the protonation of the blocks, at pH = 4 and pH = 9, respectively. Thus, in the pH region between 4 and 9, only the PMAA block is dissociated. Therefore, in this study we kept constant this initial supersaturation, the polymer concentrations were 0.05, 0.07 and 0.1 wt.% in the initial solution and pH solution was increased from 9.5, when only the PMAA block is ionized, to pH = 12, where both copolymer blocks are ionized.

The particles morphology was evidenced by SEM and AFM investigations (Figs. 1 and 2) and particles size characteristics and the average values of circularity analysis were obtained by FPIA measurements (Table 1).

As shown in Fig. 1, the surface morphology is significantly influenced by polymer concentration in the initial solution. Thus, as compared to the typical cauliflower shape of bare $CaCO_3$ particles,[7,17] at pH = 12 PHOS-*b*-PMAA induced the formation of smoother particles, of very small grain size (Fig. 1). At 0.5 wt.% initial polymer concentration small sized composite microparticles are formed (Fig. 1), with a relatively narrow size distribution (Table 1). Increasing polymer content in the initial solution, up to 0.07 and 0.1 wt.%, results in significant changes of particles characteristics, as also observed by FPIA measurements (Table 1): the particles size is non-homogeneous, with a large particle size distribution. According to SEM images (Fig. 1), smaller particles of low size distribution were obtained when composite particles where prepared at pH = 12, as compared to samples prepared at pH = 9.5.[17] These observations have been confirmed by FPIA measurements (Table 1), which gave D_{mean} values of 2 – 3.7 μm and particles mean circularity values around 0.82 – 0.89. The highest polymer charge density probably favors the formation of a denser cross-linking, involving whole polymer chains, and thus lower particle sizes are obtained.

Even if the highest magnified SEM images (Fig. 1) do not show important surface morphology changes when compared to the sample prepared at pH = 9.5,[17] the phase AFM image (Fig. 2) shows that at pH = 12 a more uniform distribution of inorganic component on particles surface is reached, without distinct domains. This is clear evidence that both ionized blocks equally contribute to particle formation, both types of ionic groups along the polymeric chain being cross-linked by calcium divalent ions.

The $CaCO_3$/PHOS-*b*-PMAA particles prepared at pH = 12 where structurally characterized to determine polymorph content (by WXD, Fig. 3a) and polymer presence into the particles (by Raman spectroscopy – Fig. 3b). Table 2 lists the XRD semi-quantitative analysis results, obtained with an EVA soft from DiffracPlus package and an ICDD-PDF2 database, based on the patterns' relative heights. The criteria used to compare simulated and measured scan was the R/R_0 ratio, where R represents the weighted reliability and R_0 is the inevitable discrepancy due to the statistics of X-ray diffraction. For an ideal fit, the R/R_0 value is 1.

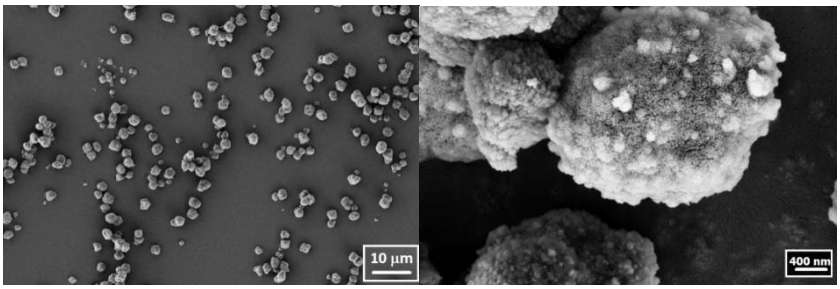

P = 0.05 wt.%

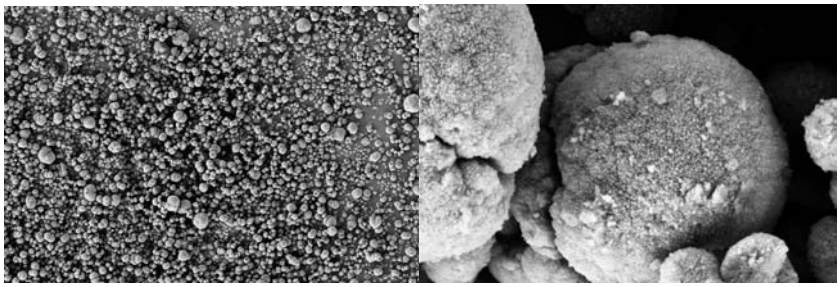

P = 0.07 wt.%

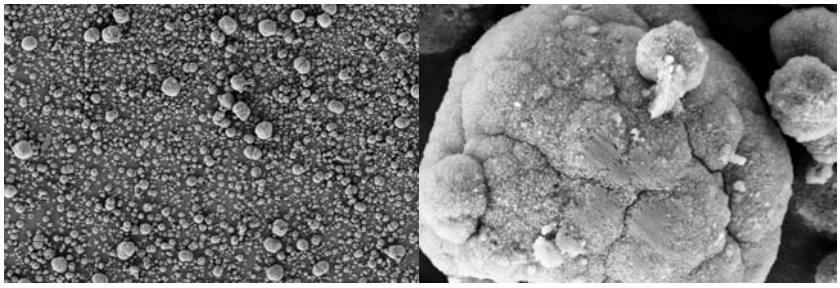

P = 0.10 wt.%

Fig. 1 – SEM images of $CaCO_3$/PHOS-*b*-PMAA particles prepared at pH = 12, using 0.2 M calcium and carbonate ions concentration and different polymer concentrations.

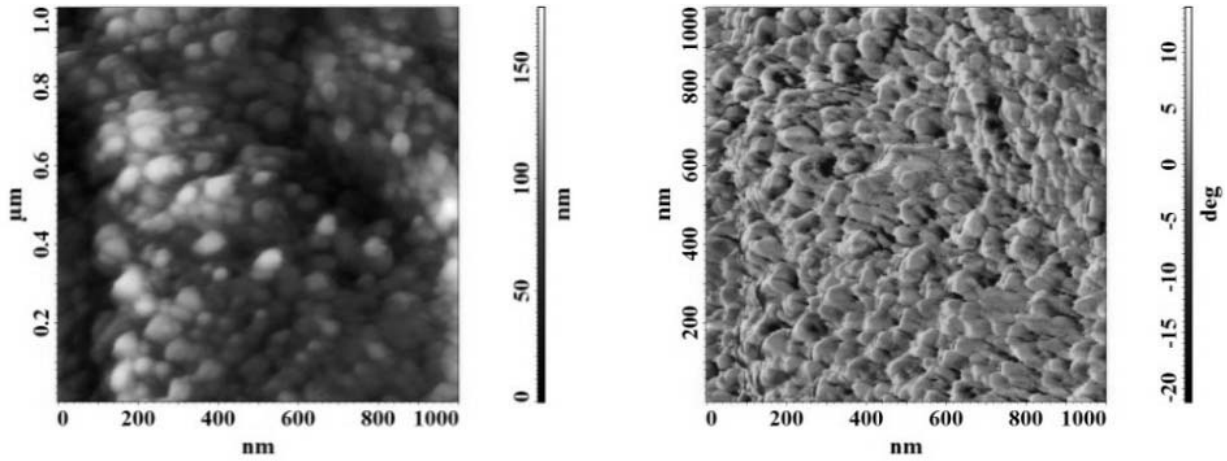

Fig. 2 – AFM height (a) and phase (b) images for the sample prepared with 0.05 wt.% PHOS-*b*-PMAA.

Table 1

Some particle size characteristics and the average values of circularity analysis of $CaCO_3$/PHOS-*b*-PMAA particles with different polymer content, obtained by FPIA measurements

Polymer concentration wt.%	D_{mean} [a] µm	C_{mean} [b]	Particle count				
			total	<5 µm	5-10 µm	10-20 µm	20-40 µm
0.05	3.69 ± 3,09 (*6.45 ± 3.9)	0.822 ± 0.146 (*0.923 ± 0.098)	1844	1671	113	57	3
0.07	2.03 ± 2.32 (*3.62 ± 2.1)	0.878 ± 0.124 (*0.767 ± 0.095)	2290	2183	86	20	1
0.10	1.94 ± 2.80 (*2.29 ± 1.6)	0.890 ± 0.122 (*0.774 ± 0.129)	2433	2299	98	32	4

[a]mean diameter; [b]mean particles' circularity
*values obtained when crystallization took place at pH = 9.5[17]

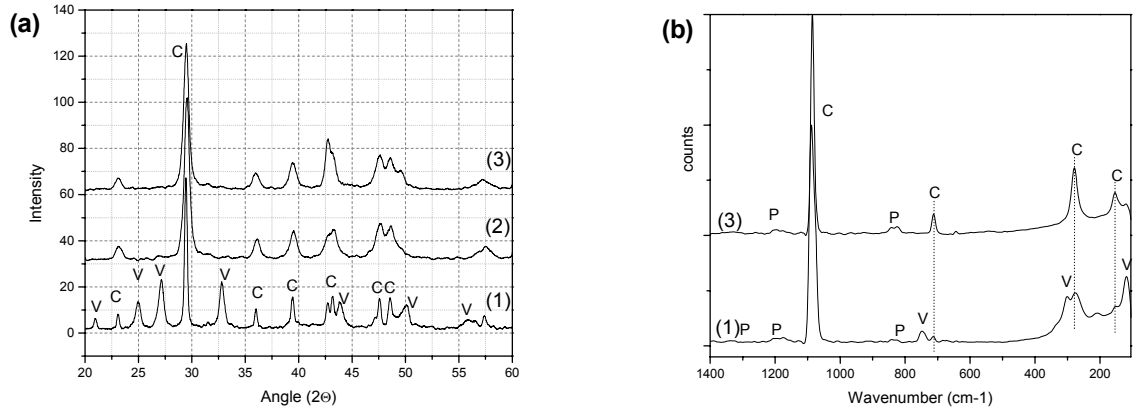

Fig. 3 – (a) XRD diffractograms and (b) Raman spectra of $CaCO_3$/PHOS-*b*-PMAA microparticles, prepared with different polymer concentrations; (1) 0.05 wt.%, (2) 0.07 wt.%, (3) 0.10 wt.%

Table 2

XRD semi-quantitative analysis of $CaCO_3$/PHOS-*b*-PMAA, using an ICDD-PDF2 database

Polymer concentration, wt.%	Polymorph ratio, %		Crystallite Size (Scherrer), Å		R/R_0
	calcite	vaterite	calcite	vaterite	
0.05	63.5 (*54.8)	36.5 (*45.2)	176.0	258.7	1.03
0.07	96.5 (*6.5)	3.5 (*93.5)	159.0	280.9	1.02
0.10	95.4 (*7.8)	4.6 (*92.2)	157.7	330.1	1.05

* values obtained when crystallization took place at pH = 9.5[17]

As Fig. 3 shows, both calcite and vaterite polymorphs are present in particles structure. The lattice constants for each detected polymorph were not influenced by the ratio between polymorph fraction or polymer presence, and were the same with that of the samples prepared without polymer[7]: a = b = 4.988 Å and c = 17.061 Å for calcite and a = b = 7.147 Å and c = 16.917 Å for vaterite. The increase of polymer content favors the formation of calcite and inhibits vaterite formation when polymer content is higher than 0.07 wt.%. This behavior is completely opposite to that of particles obtained with the same polymer content at pH = 9.5,[17] when vaterite is the main formed polymorph. According to previous reports,[6,17-20] the presence of carboxylate groups favors vaterite formation. The formation of calcite at pH = 12 can be ascribed to a synergistic effect of both protonated OH groups of p-hydroxystyrene block and the ionic species (HCO_3^- or CO_3^{2-})

formed as a function of pH. Previous studies show that above pH = 10, carbonate ions become the dominant species in the reaction mixture and favor calcite formation.[21,22] The same polymorph content was observed in the Raman spectra (Fig. 3b).

Polymer presence in composite particles was quantified from the thermal degradation of the composite particles up to 540 °C (Fig. 4, Table 3).

Thus, taking into account the 4.27 wt.% weight loss up to 540 °C and the amount of polymer used in the initial mixture, 4.76 wt.% of total components, it appears that about 89% of polymer has been included in the composite material when 0.05 wt.% PHOS-*b*-PMAA was used in the initial reaction mixture, close but lower than the included polymeric amount when the pH was 9.5.[17] The amount of included polymer decreases with the polymer amount used in the initial mixture, in agreement with but lower than the results obtained at pH = 9.5.

The presence of PHOS-*b*-PMAA on and into $CaCO_3$ microparticles has been confirmed by the electrokinetic characterization (Table 4).

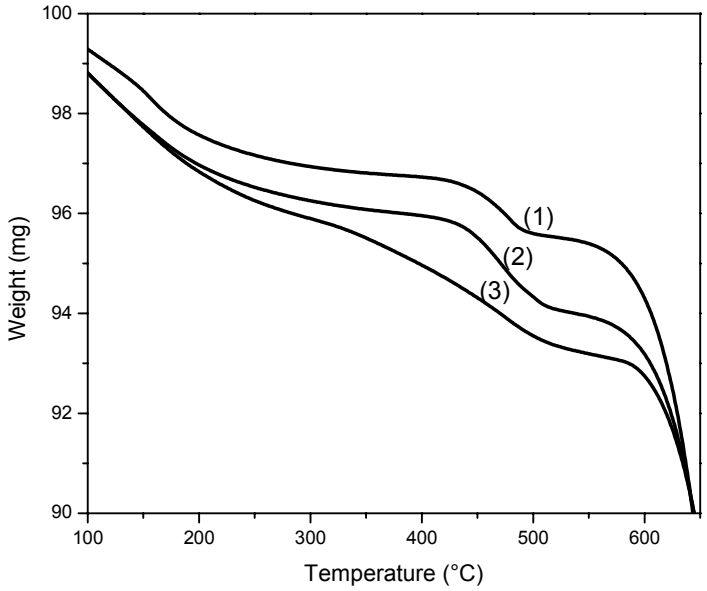

Fig. 4 – TGA plots of $CaCO_3$/PHOS-*b*-PMAA composites with various contents in block copolymer; (1) 0.05 wt.%, (2) 0.07 wt.%, (3) 0.10 wt.%

Table 3

TGA results of $CaCO_3$/PHOS-*b*-PMAA composites with various contents in block copolymer

Polymer concentration, wt.%	W,[a] wt.%	P_i,[b] wt.%	P_r,[c] %
0.05	4.27	4.76	89.73 (*96)
0.07	5.22	6.54	79.79 (*82)
0.10	6.31	9.09	69.45 (*73)

a – weight loss up to 540 °C; b – polymer used in initial mixture as wt.% of total components; c – polymer included in composite material, $P_r = W/P_i \times 100$

* values obtained when crystallization took place at pH = 9.5[17]

Table 4

Some $CaCO_3$/PHOS-*b*-PMAA particles characteristics at pH 5.5

Polymer concentration, wt.%	Charge density, meq/g	Zeta potential, mV
0.05	-19.38 (*-16.37)	-28.7 ± 0.43 (*-22.6 ± 2.39)
0.07	-18.84 (*-12.03)	-25.9 ± 0.52 (*-18.7 ± 0.45)
0.10	-16,38 (*-10.99)	-22.1 ± 0.77 (*-12.2 ± 0.62)

*values obtained when crystallization took place at pH = 9.5[17]

The electrokinetic measurements revealed an increase of particles' charge density and zeta potential with increasing polymer amount as compared to the corresponding samples prepared at pH = 9.5, due to a higher polymer charge density (-78.4 meq/g at pH = 12). The microparticles prepared at a 0.05 wt.% polymer concentration show a small increase of charge density and zeta potential as compared to bare $CaCO_3$ particles.[17] This behavior suggests that the polymer has been homogeneously embedded into composite particles, whereas at higher polymer concentrations (0.07 and 0.1 wt.%) the polymeric micelle features in the particles lead to less free charges on the surface.

EXPERIMENTAL

Materials

$CaCl_2 \cdot 2\ H_2O$ and Na_2CO_3 from Sigma-Aldrich were used as received. The PHOS-*b*-PMAA block copolymer was synthesized and purified as previously described.[15] Briefly, *t*-butoxy styrene was polymerized first under high vacuum using anionic polymerization. The growth of the second block, namely poly(*t*-butyl methacrylate) took place by addition of the respective monomer. The formed block copolymer was isolated by precipitation and was subsequently hydrolyzed in acidic conditions to remove the tert-butyl protective groups of both blocks. The molecular characteristics of the block copolymer are M_w = 15400 and wt.% PHOS = 30.[15]

Preparation of $CaCO_3$/PHOS-*b*-PMAA composite microparticles

The formation of $CaCO_3$/PHOS-*b*-PMAA composites was carried out in glass beakers, at about 22 ^oC. Aqueous solutions with different PHOS-*b*-PMAA concentrations were first prepared (0.05, 0.07 and 0.1 wt.%) and then specific amounts of Na_2CO_3 were dissolved into copolymer solutions to get an inorganic concentration of 0.2 M. Equal volumes of as prepared solutions and 0.2 M $CaCl_2$ aqueous solutions were rapidly mixed. The pH of the mixtures was about 9.5 and was adjusted to 12 immediately after components mixing. The mixtures were stirred for 1 min on a magnetic stirrer, at room temperature, and then the dispersions were kept under static conditions for 60 min. The obtained microparticles were separated by filtration, intensively washed with water and finally washed with acetone and dried in an oven at 40 ^oC.

Characterization of $CaCO_3$/PHOS-*b*-PMAA composite microparticles

The particles shape and surface were examined using a Scanning Electron Microscope type Ultra plus (Carl Zeiss NTS), operating at 4 kV with secondary electrons, in high vacuum mode. For a better resolution the particles were sputtered with platinum. The study of some composite particles surface was performed by a Scanning Probe Microscope Solver Pro-M (NT-MDT Co, Zelenograd, Russia) in the configuration of an atomic force microscope. The images were obtained in semicontact mode, in air, using a NSG 03 silicon cantilever with the length of 135 μm, resonant frequency of 93 kHz and tip radius of curvature less than 10 nm. The particles size, size distribution and their circularity has been evaluated using the Sysmex Dynamic Flow Particle Image Analyzer 2100. To obtain correct values, the Sysmex FPIA 2100 image analyzer was checked before starting the main experiment by using certified size standards.

The characterization of the samples was carried out using X-ray diffraction (D8 Advance Bruker AXS). The X-rays were generated using a Cu K_α source with an emission current of 36 mA and a voltage of 30 kV. Scans were collected over the $2\theta = 20 – 60°$ range using a step size of 0.01° and a count time of 0.5 s/step. The semi-quantitative analysis was performed with an EVA soft from DiffracPlus package and an ICDD-PDF2 database, based on patterns' relative heights. The chemical composition of carbonate/polymer microparticles was evaluated by Raman spectroscopy by using a Renishaw inVia Raman Spectrometer equipped with a Leica microscope with 5x and 100x objectives (acquisition time 10 minutes). The range of vibration frequencies was from 100 to 1500 cm^{-1}. The 514.5 nm line of an Ar^+ laser was used for excitation at a power of ~0.7 mW (100%).

Thermogravimetric analysis has been performed using a TGA Q500 V20.2 Build 27 instrument, in an inert atmosphere of nitrogen. In a typical experiment ~20 mg of material were placed in the sample pan and the temperature was equilibrated at 60 ^oC. Subsequently, the temperature was increased to 700 ^oC with a rate of 10 ^oC/min and the weight changes were recorded as a function of temperature.

The electrokinetic potential of carbonate particle dispersions was measured with a ZetaSizer Nano ZS (Malvern, UK) operating at the wavelength 633 nm. The equipment measures the electrophoretic mobility of the particles, and converts it into the zeta potential, using the von Smoluchowski equation. The results were expressed as the average of at least five independent measurements performed on 0.5 mg/ml aqueous dispersions, for each sample.

CONCLUSIONS

In this study, calcium carbonate microspheres templated by the PHOS-*b*-PMAA block-copolymer were obtained. The initial solution pH and thus the type of formed ions in the reaction mixture (polymer completely ionized and carbonate ions as the dominant species in the reaction mixture) had a remarkable effect on the morphology and polymorphism of $CaCO_3$ particles. SEM images show that large size distribution of spherical aggregates were obtained for all tested polymer concentrations. At pH = 12 both copolymer blocks are in the ionized form, this favoring the formation of a dense crosslinking involving the whole polymer chains. The phase AFM image shows a uniform distribution of inorganic component on particle surface, without distinct domains. The increase of polymer content favors the formation of calcite due to a synergistic effect of protonated

OH groups of *p*-hydroxystyrene block and the carbonate ions that are the dominant species in the reaction mixture and favor calcite formation. This study emphasizes the role of reaction medium pH on the characteristics of the formed composite microparticles, as a valuable parameter to tune microparticle size and the polymorphs content.

Acknowledgement: This work was supported by a grant of the Roumanian National Authority for Scientific Research and Innovation, CNCS – UEFISCDI, project number PN-II-RU-TE-2014-4-1433.

REFERENCES

1. R. A. Ahmeda, A. M. Fekryc and R. A. Farghalia, *Appl. Surf. Sci. B,* **2013**, *285*, 309-316.
2. K. Ahmad, I. A Bhatti, M. Muneer, M. Iqbal and Z. Iqbal, *IJCBS*, **2012**, *2*, 248-253.
3. S. B. Mukkamala, C. E. Anson and A. K. Powell, *J. Inorg. Biochem*., **2006**, *100*, 1128-1138.
4. J. Yu, M. Lei, B. Cheng and X. Zhao, *J. Solid State Chem*., **2004**, *177*, 681-689.
5. C. Y. Tai, W. C. Chien and J. P. Hsu, *AIChEJ*, **2005**, *51*, 480-486.
6. M. Mihai, F. Bucătariu, M. Aflori and S. Schwarz, *J. Cryst. Growth*, **2012**, *351*, 23-31.
7. M. Mihai, M.-D. Damaceanu, M. Aflori and S. Schwarz, *Cryst. Growth Des*., **2012**, *12*, 4479-4486.
8. F. Doroftei, M.-D. Damaceanu, B. C. Simionescu and M. Mihai, *Acta Cryst.*, **2014**, *B70*, 227-235.
9. M. Mihai, C. Steinbach, M. Aflori and S. Schwarz, *Mater. Design*, **2015**, *86*, 388-396.
10. S. Zhang, *Nature Biotechnology*, **2003**, *21*, 1171-1178.
11. A. Rosler, G. W. Vandermeulen and H. A. Klok, *Adv. Drug Deliv. Rev.*, **2001**, *53*, 95-108.
12. H. Colfen and L. Qi, *Chem. Eur. J.*, **2001**, *7*, 106-116.
13. M. Ogris, G. Walker, T. Blessing, R. Kircheis, M. Wolschek and E. Wagner, *J. Controll. Release*, **2003**, *91*, 173-181.
14. B. Jeong and A. Gutowska, *Trends in Biotechnology*, **2002**, *20*, 305-311.
15. G. Mountrichas and S. Pispas, *Macromolecules*, **2006**, *39*, 4767-4774.
16. B. P. Bastakoti, S. Guragain, Y. Yokoyama, S.-i. Yusa and K. Nakashima, *Langmuir*, **2011**, *27*, 379-384.
17. M. Mihai, G. Mountrichas, S. Pispas, I. Stoica, M. Aflori, M. Auf der Landwehr, I. Neda and S. Schwarz, *J. Appl. Cryst*., **2013**, 46, 1455-1466.
18. M. Mihai, I. Bunia, F. Doroftei, C.-D. Varganici and B.C. Simionescu, *Chem. Eur. J*., **2015**, *21*, 5220-5230.
19. A. Barhoum, H. Rahier, R. E. Abou-Zaied, M. Rehan, T. Dufour, G. Hill and A. Dufresne, *ACS Appl. Mater. Interf*., **2014**, *6*, 2734-2744.
20. S.-C.Huang, K. Naka and Y. A Chujo, *Langmuir*, **2007**, *23*, 12086-12095.
21. M. F. Butler, W. J. Frith, C. Rawlins, A. C. Weaver and M. Heppenstall-Butler, *Cryst. Growth Des*., **2009**, *9*, 534-545.
22. J. Yu, H. Guo, S. A. Davis and S. Mann, *Adv. Funct. Mater.*, **2006**, *16*, 2035-2041.